Colloid Polym Sci 280:380–388 (2002)

ORIGINAL CONTRIBUTION

Kenichi Izawa
Toshiaki Ogasawara
Hideki Masuda
Hirofumi Okabayashi
Charmian J. O'Connor
Isao Noda

Growth process of polymer aggregates formed by perfluorooctyltriethoxysilane. Time-resolved near-IR and two-dimensional near-IR correlation studies

Received: 25 July 2001
Accepted: 16 October 2001

K. Izawa
Fuji Silysia Chemical Ltd., Nakatsugawa Technical Center, 1683-1880 Nakagaito Nasubigawa, Nakatsugawa
Gifu 509-9132, Japan

T. Ogasawara
Tokai Technical Center Foundation
710, Inokoshi 2, Meito-ku, Nagoya
Aichi 465-0021, Japan

H. Masuda · H. Okabayashi (✉)
Department of Applied Chemistry
Nagoya Institute of Technology
Gokiso-cho, Showa-ku
Nagoya, Aichi 466-8555, Japan

C. J. O'Connor
Department of Chemistry, The University of Auckland, Private Bag 92019, Auckland
New Zealand

I. Noda
The Procter and Gamble Company
8611 Beckett Road, West Chester
OH 45069, USA

Abstract The polymerization of 1*H*, 1*H*, 2*H*, 2*H*-perfluorooctyltriethoxysilane in ethanol, catalyzed by 0.5, 1.0 and 2.0 M $HCl{\cdot}H_2O$, has been examined using time-resolved near-IR (NIR) and 2D NIR correlation techniques. The time-resolved NIR results have demonstrated that the growth of polymeric aggregates prior to the phase separation proceeds in a two-step process, which depends upon the HCl concentration. Furthermore, it has been found that the 2D NIR correlation data provide direct information on the sequence of the intricate reaction steps and interaction of participating components through hydrogen bonding in the growth process.

Keywords Polymer aggregates · Perfluorooctyltriethoxysilane · Time-resolved NIR · 2D NIR correlation

Introduction

Hydrolysis of silane alkoxide or alkyl alkoxide brings about the formation of silanols which subsequently condense to form polymers. The nature of the polymeric species produced by acid catalysis is different from that of the base-catalyzed products. This difference may be explained by three reaction factors [1]: differences in the relative rates of hydrolysis of the alkoxide or alkyl alkoxide species to form silanols; condensation of silanols to form the polymer; linking of the polymeric species produced. These factors are strongly dependent upon the concentration of water and alkoxide or alkyl alkoxide and the pH of the solution [1, 2]. Detailed understanding of these factors in the reaction system is of critical importance, and will lead to further development of various applications in the industrial arena.

The extremely bulky and rigid perfluorooctyl (PFO) segment of a 1*H*, 1*H*, 2*H*, 2*H*-perfluorooctyltriethoxysilane (PFOTES) molecule has little interaction with water molecules because it has characteristics of both hydrophobicity and lipophobicity [3]. We may therefore expect that the PFO chains self-assemble during polymerization

of the PFOTES–substrate system, leading to the formation of a giant aggregate. Such self-assembling behavior of the PFO chains should be reflected in the microstructural variation of the polymeric aggregates.

Recently, we investigated the time-resolved small-angle X-ray scattering (SAXS) data, using Guinier's law [4, 5], for the polymerization process in the PFOTES–ethanol system catalyzed at different HCl concentrations. The result showed that the growth of the polymeric aggregates prior to the phase separation proceeds in a two-step process, in which the formation of small clusters occurs in the initial step, while in the second step much larger clusters are formed.

In the present study, time-resolved near-IR (NIR) and 2D NIR correlation spectra were used to examine the microstructural variation in the reaction of the PFOES–ethanol–$HCl{\cdot}H_2O$ system over a time period of 10–240 min. In particular, the HCl-concentration dependence of the 2D NIR correlation spectra was examined in detail, since the HCl concentration is strongly related to the reaction factors mentioned previously.

2D correlation spectroscopy, which was first proposed by Noda [6–9] as a novel analytical technique based on time-resolved detection of IR absorption signals, has been used to elucidate various chemical interactions. Its application has been successfully extended to a variety of areas, including NIR studies [10–12]. In our previous work [13, 14], we have already demonstrated that the subtle details of NIR spectroscopic features of polymerization process of alkyl alkoxides are markedly reflected in the 2D NIR correlation spectra.

Experimental

Materials

PFOTES was purchased from Lancaster Synthesis, UK, and was used without further purification. Ethanol was chosen as a solvent, and the 0.5, 1.0 and 2.0 M $HCl{\cdot}H_2O$ systems were used as catalysts.

Time-resolved NIR spectral measurements

Time-resolved NIR spectra of a one-phase solution sample were recorded until phase separation occurred at a resolution of 8 cm^{-1} using a Nicolet Magna System 860 Fourier transform IR Spectrometer (4,000–10,000 cm^{-1}) equipped with a deuterated triglyceride sulfate KBr detector at room temperature (298 K). The sample solution was sandwiched between two CaF_2 windows using a Pb spacer (0.2 mm). Forty scans were accumulated to ensure an acceptable signal-to-noise ratio. A total of 800 time-resolved NIR spectra for each of the PFOTES–ethanol–$HCl{\cdot}H_2O$ (0.5, 1.0 and 2.0 M) systems were observed.

2D NIR correlation analysis

Synchronous and asynchronous 2D NIR correlation spectra were generated from the time-resolved NIR spectral data, using the generalized 2D correlation scheme [9]. The basic mathematical procedure for obtaining a 2D correlation map was described in recent publications [15, 16]. Computation was carried out using the 2D-OGAIZA software developed at the Nagoya Institute of Technology.

Results

Time-resolved NIR spectra and HCl-concentration dependence

The NIR spectrum of the PFOTES–ethanol–0.5 M $HCl{\cdot}H_2O$ system in the 4,000–7,500 cm^{-1} region, which was measured about 90 s after mixing the sample, is shown in Fig. 1. Most of the NIR bands in this region come mainly from the combination [ν(CH) + $\delta(CH_2)$] modes between the CH_3 or CH_2 stretching [ν(CH)] and bending [$\delta(CH_2)$] modes, in addition to the bands arising from water [13, 14, 16]. Therefore, in this region of the NIR spectra of the PFOTES–ethanol–$HCl{\cdot}H_2O$ system, a $(CH_2)_2$ group of the PFO segment, the three CH_3CH_2O groups and ethanol contribute to the bands. Since the condensation and hydrolysis reactions bring about the time-dependent release of water and ethanol, respectively, the NIR bands coming from released water and ethanol increase in intensity. The band at 4,818 cm^{-1} is assigned to the combination mode between the alcohol OH stretching and bending modes of the added ethanol and of the ethanol

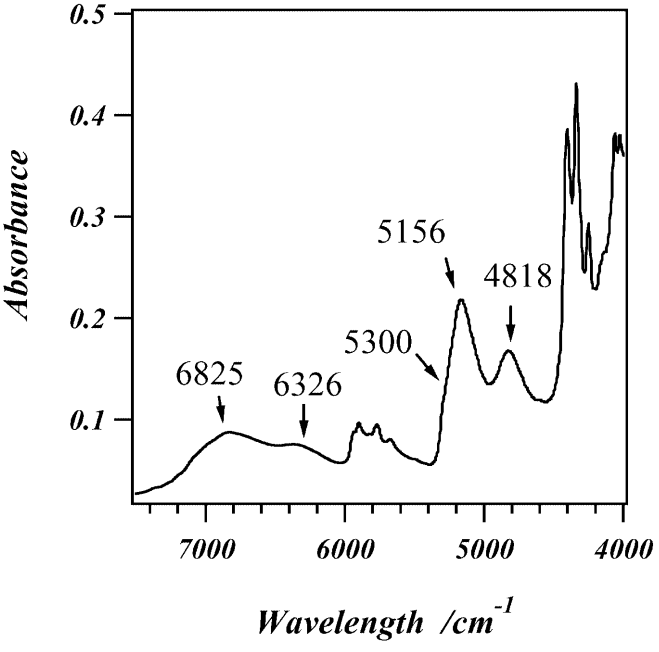

Fig. 1 Near-IR spectrum in the 4,000–7,500 cm^{-1} region for the perfluorooctyltriethoxysilane (*PFOTES*)–ethanol–0.5M $HCl{\cdot}H_2O$ system

released as a consequence of hydrolysis [13]. The band at 5,156 cm^{-1} arises from the H_2O molecules and is ascribed to the combination modes ($\nu_2 + \nu_3$) between the H_2O deformation (ν_2) and H_2O asymmetric stretching (ν_3) modes. The shoulder band at about 5,300 cm^{-1} comes from the combination modes between the SiOH stretch mode (ν) and the overtone of the SiOH bending mode (δ) [13]. The very broad bands at 6,326 and 6,825 cm^{-1} also come from the overtone modes of alcohol and water OH groups.

We measured the time-resolved NIR spectra of the reaction process for the PFOTES–ethanol–$HCl{\cdot}H_2O$ system. The time dependence of absorption for the 5,156 and 4,818-cm^{-1} bands was examined at different HCl concentrations (0.5, 1.0 and 2.0 M). It was found that the absorbance of the NIR bands at 4,818 and 5,156 cm^{-1}, as well as those at 6,326 and 6,825 cm^{-1}, depends upon the reaction time and the HCl concentration, indicating that both the time and the HCl-concentration dependence of these bands reflect the reaction processes of hydrolysis and condensation. The increase in absorbance for the 4,818-cm^{-1} band implies the liberation of ethanol produced from the hydrolysis, and that for the 5,156-cm^{-1} band reflects the presence of water molecules released as a consequence of condensation to form a siloxane bond.

The time dependence of absorbance for the 5,156-cm^{-1} band is shown in Fig. 2a. We point out that variation in absorbance for this NIR band occurs in a two-step process (I and II). For the 0.5 M HCl-catalyzed sample, the absorbance of the 5,156-cm^{-1} band increases during the earlier initial step I (600–800 s); however, it tends to converge to a constant value in the later part of the initial step (800–9,300 s). In step II (later than 9,300 s), the absorbance rapidly increases and then tends to stabilize. We may regard the time of 9,300 s as the commencement time for step II. For the 1.0 M $HCl{\cdot}H_2O$-catalyzed system, a similar time dependence was found, and the time for commencement of step II is 5,300 s. However, for the 2.0 M $HCl{\cdot}H_2O$-catalyzed system, we find that such a time-dependent variation of absorbance occurs more rapidly (the commencement time for step II is 2,000 s). Unfortunately, for this concentrated HCl-catalyzed system, we could not confirm the convergence of the 5,156-cm^{-1} absorbance to a constant value, since phase separation occurred. Thus, liberation of ethanol and water rapidly occurs in the second step, and an increase in the HCl concentration evidently promotes the time for commencement of the second process.

The time dependence of absorption for the 4,818-cm^{-1} band is shown in Fig. 2b. We find that the variation of absorbance for this band also occurs in a two-step process, and the time for the commencement of step II is the same as that obtained using the 5,156-cm^{-1} band.

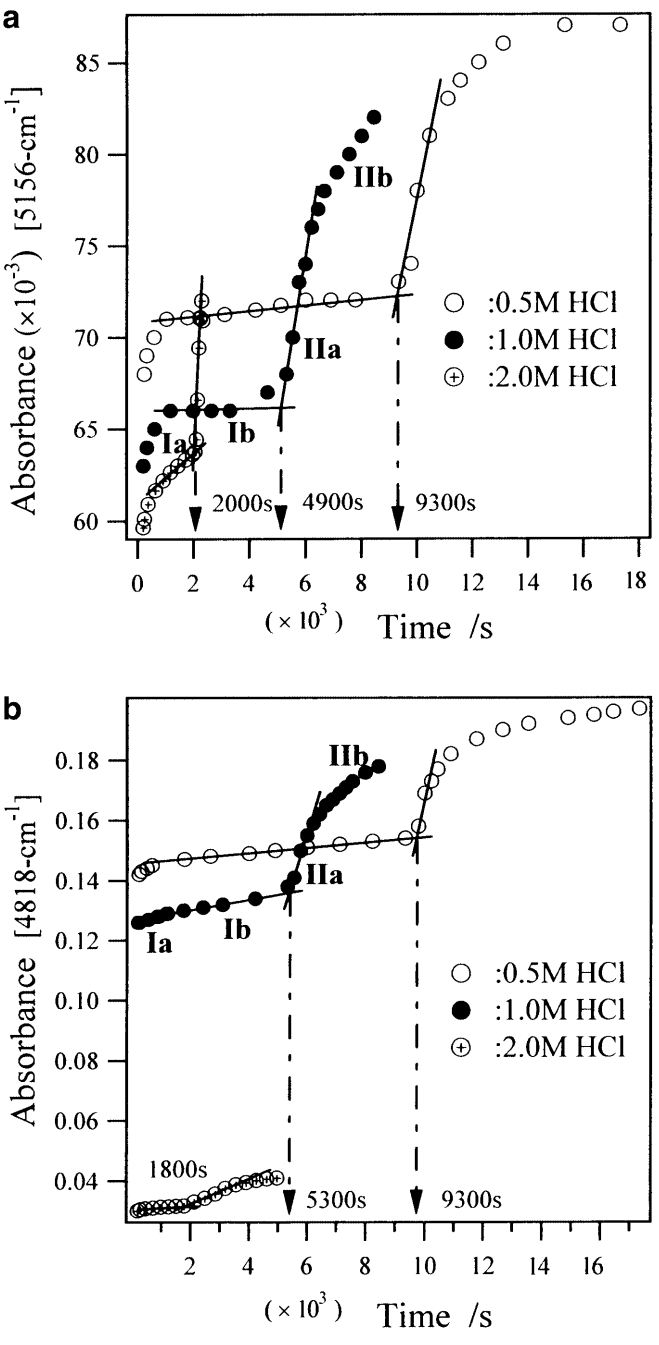

Fig. 2 Time-dependence of absorbance for **a** the 5,156-cm^{-1} band and **b** the 4,818-cm^{-1} band at different HCl concentrations: 0.5 M (*open circles*), 1.0 M (*filled circles*), and 2.0 M (*crossed circles*)

Recently, we examined the HCl-concentration dependence of SAXS spectra for the same sample systems, catalyzed by 0.5, 1.0 and 2.0 M $HCl{\cdot}H_2O$. The time dependence of the apparent radius of gyration, obtained from Guinier plots, showed that the growth of the polymer aggregates occurs in a two-step process. Small clusters involving monomers, dimers, and trimers are formed in step I, and formation of larger clusters occurs

in the step II. Furthermore, we have confirmed that a higher HCl concentration also promotes the time for commencement of step II.

2D NIR correlation and its HCl-concentration dependence

For further understanding of the two-step reaction mechanism, the 2D NIR correlation spectra were calculated from the time-resolved NIR spectra of the PFOTES–ethanol samples catalyzed by 1.0 M HCl·H_2O. In order to examine the time-dependent 2D NIR correlation spectra in detail, steps I and II are classified as I_a for an initial rise in absorbance (200–600 s) and I_b for the plateau region (1,200–3,400 s) and as II_a for the second rapid increase (5,300–6,000 s) and II_b for the slow increase (6,600–8,000 s). In particular, we focused our attention on the region of 4,600–5,400 cm^{-1}, which can be used to discuss the OH vibrational modes of alcohol, water, and silanol.

The 2D NIR correlation spectra are shown in Figs. 3 and 4. The coordinates and signs of the correlation peaks in the synchronous maps are summarized in Table 1. The order of events corresponding to the individual cross peaks, which is obtained from the asynchronous maps using the general peak sign rule described in Ref. [9], is listed in Tables 2 and 3.

In the synchronous correlation spectrum (step I_a) (Fig. 3a, right), we find three autopeaks at the diagonal coordinates A_1 ($\nu_1 = \nu_2 = 5{,}280$), A_2 (5,107) and A_3 (4,748), four positive cross peaks at the off-diagonal positions of coordinates B_1 ($\nu_1 = 4{,}860$, $\nu_2 = 5{,}280$), B_2 (4,748, 5,280), B_3 (5,280, 4,860) and B_4 (5,280, 4,748), and two negative cross peaks at coordinates C_1 ($\nu_1 = 5{,}107$, $\nu_2 = 5{,}280$) and C_2 (5,280, 5,107). We can construct a synchronous correlation square by linking the two autopeaks (A_1 and A_2) with the two negative

Fig. 3 Synchronous (top) and asynchronous (bottom) correlation maps of the PFOTES–ethanol–1.0M HCl·H_2O system for **a** step I_a (200–600 s) and for **b** step I_b (1,200–3,400 s)

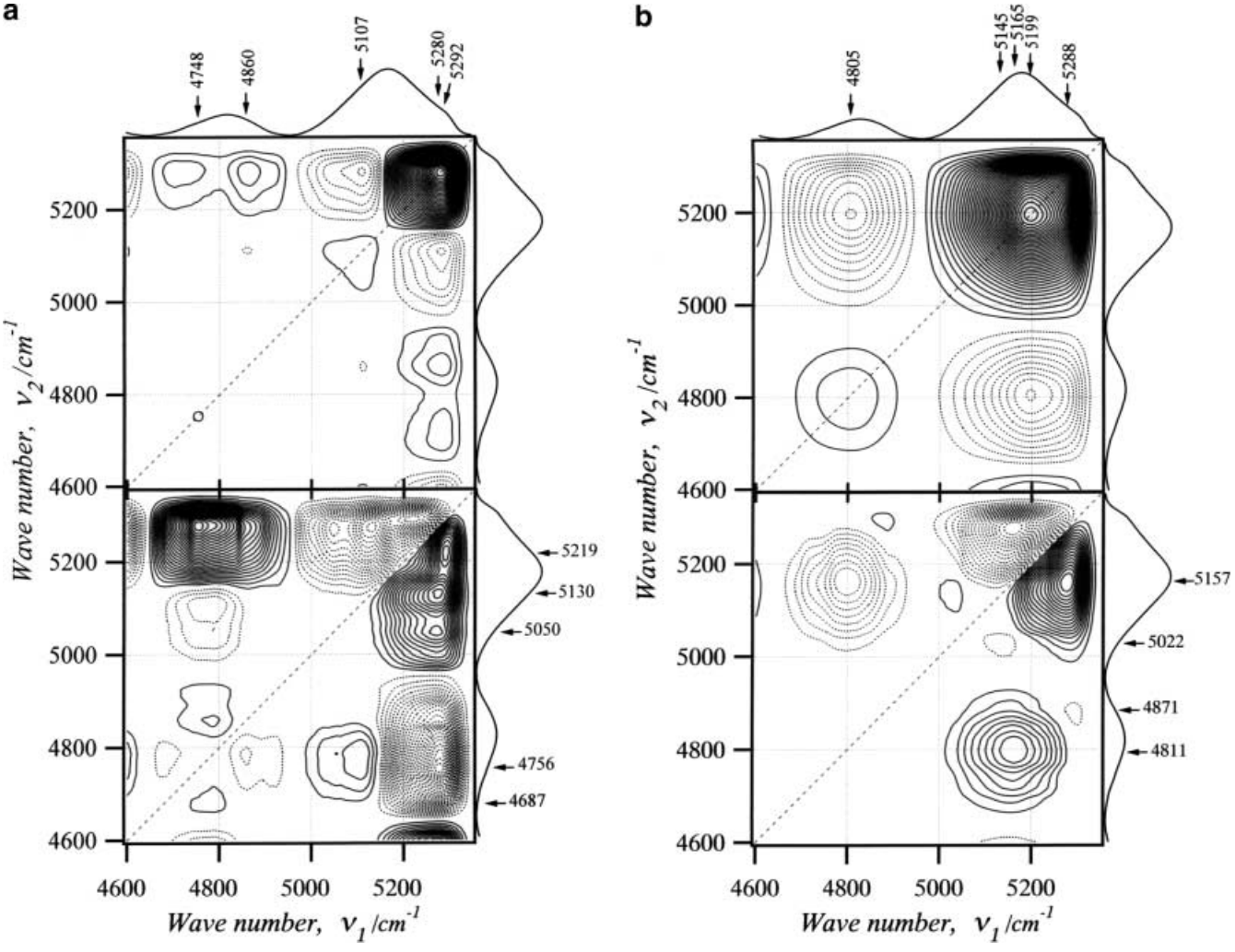

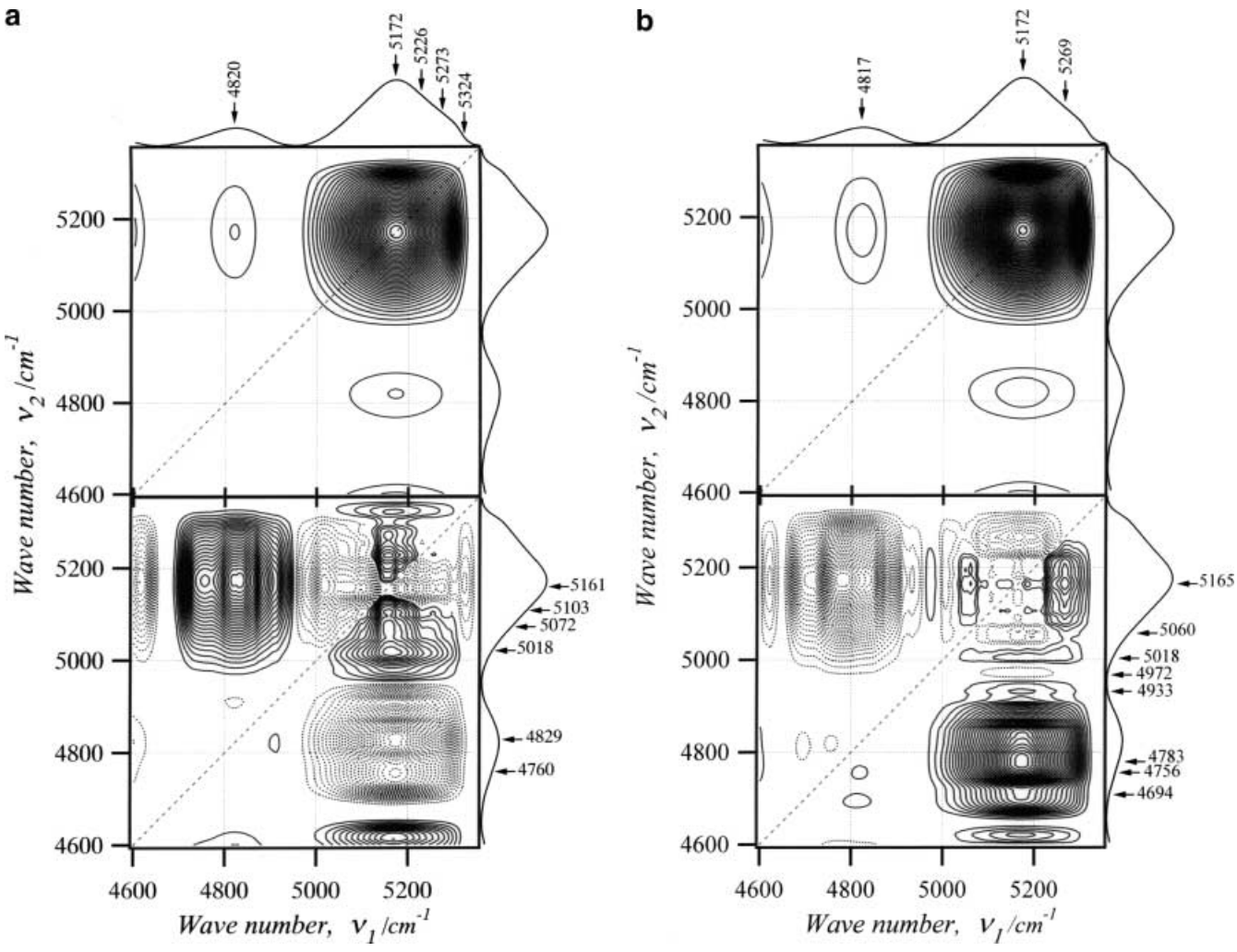

Fig. 4 Synchronous (top) and asynchronous (bottom) correlation maps of the PFOTES–ethanol–1.0M HCl·H_2O system for **a** step II_a (5,300–6,000 s) and for **b** step II_b (6,600–8,000 s)

cross peaks (C_1 and C_2). Therefore, there is a correlation between the two NIR bands at 5,280 and 5,107 cm^{-1}, which arise from the $\nu + 2\delta$ combination modes of a SiOH group and the $\nu_2 + \nu_3$ combination modes of a H_2O molecule, respectively. We may assign the two bands at 5,280 and 5,107 cm^{-1} to associated silanol and strongly hydrogen-bonded water, respectively, on the basis of results of previous studies [13, 14]. This correlation square implies the existence of association between water and silanol. The very strong intensity of autopeak A_1 reflects that monomers with silanol groups are produced rapidly as a consequence of hydrolysis in step I_a. The negative signs of cross peaks C_1 and C_2, with relatively high correlation intensity levels, reflect the difference in the extent of the time dependence of the intensity between the bands at 5,280 and 5,107 cm^{-1}, i.e., the extent of the intensity increase of the band at 5,107 cm^{-1} is smaller than that for the band at 5,280 cm^{-1}. The cross peaks B_i ($i = 1$–4) evidently arise from the correlation of the alcohol 4,860-cm^{-1} (or 4,748-cm^{-1}) band with the silanol 5,280-cm^{-1} band through hydrogen bonding, since we may assign the 4,860 and 4,748-cm^{-1} bands to weakly and strongly associated alcohol OH groups, respectively.

Table 1. Coordinates of synchronous autopeaks and cross peaks at each step

Synchronous peak	Step	Peak Position
Autopeak ($\nu_1 = \nu_2$)	I_a	A_1 (5,280), A_2 (5,107), A_3 (4,748)
	I_b	A_1 (5,199), A_2 (4,805)
	II_a	A_1 (5,172)
	II_b	A_1 (5,172)
Cross peak ($\nu_1 = \nu_2$)	I_a	B_1 (4,860, 5,280), B_2 (4,748, 5,280), B_3 (5,280, 4,860), B_4 (5,280, 4,748) C_1 (5,107, 5,280), C_2 (5,280, 5,107)
	I_b	C_1 (4,805, 5,199), C_2 (5,199, 4,805)
	II_a	B_1 (4,820, 5,170), B_2 (5,170, 4,820)
	II_b	B_1 (4,817, 5,172), B_2 (5,170, 4,817)

Table 2 Coordinates and signs of asynchronous cross peaks in steps I_a and I_b with order of events. $v_x \rightarrow v_y$: the event of v_x occurs before that of v_y

Asynchronous cross peak (v_1, v_2)	Sign		Order of events
	Φ synchronous intensity	Ψ asynchronous intensity	
Step I_a			
S_w (5,292, 5,219)	+	+	$v_1 \rightarrow v_2$
S_H (5,292, 5,130)	–	+	$v_2 \rightarrow v_1$
S'_H (5,280, 5,050)	–	+	$v_2 \rightarrow v_1$
S_{Al} (5,280, 4,650–4,950)	+	–	$v_1 \rightarrow v_2$
W_{Al} (5,107, 4,756)	–	+	$v_2 \rightarrow v_1$
E_w (4,860, 4,783)	+	–	$v_1 \rightarrow v_2$
Al_s (4,748, 4,687)	+	–	$v_1 \rightarrow v_2$
Step I_b			
S'_w (5,288, 5,157)	+	+	$v_1 \rightarrow v_2$
S_{Al} (5,288, 4,871)	–	–	$v_2 \rightarrow v_1$
W_S (5,145, 5,022)	–	–	$v_2 \rightarrow v_1$
W'_{Al} (5,165, 4,811)	–	+	$v_2 \rightarrow v_1$

Table 3 Coordinates and signs of asynchronous cross peaks in steps II_a and II_b with order of events. $v_x \rightarrow v_y$: the event of v_x occurs before that of v_y

Asynchronous cross peak (v_1, v_2)	Sign		Order of events
	Φ synchronous intensity	Ψ asynchronous intensity	
Step I_a			
S_1 (5,324, 5,161)	+	–	$v_1 \rightarrow v_2$
S_2 (5,273, 5,161)	+	–	$v_1 \rightarrow v_2$
S'_H (5,226, 5,161)	+	–	$v_1 \rightarrow v_2$
W_1 (5,157, 5,103)	+	+	$v_1 \rightarrow v_2$
W_2 (5,157, 5,072)	+	+	$v_1 \rightarrow v_2$
W_3 (5,157, 5,018)	+	+	$v_1 \rightarrow v_2$
Al_1 (5,170, 4,829)	+	–	$v_1 \rightarrow v_2$
Al_2 (5,170, 4,760)	+	–	$v_1 \rightarrow v_2$
Step I_b			
S'_2 (5,269, 5,165)	+	+	$v_1 \rightarrow v_2$
W'_1 (5,269, 5,018)	+	+	$v_1 \rightarrow v_2$
W'_2 (5,170, 5,060)	+	–	$v_1 \rightarrow v_2$
W'_3 (5,170, 4,972)	+	–	$v_1 \rightarrow v_2$
W''_1 (5,170, 4,933)	+	+	$v_1 \rightarrow v_2$
W''_2 (5,170, 4,817)	+	+	$v_1 \rightarrow v_2$
W''_3 (5,170, 4,783)	+	+	$v_1 \rightarrow v_2$
W'_4 (5,170, 4,694)	+	+	$v_1 \rightarrow v_2$

The corresponding asynchronous spectrum (step I_a) is shown in Fig. 3a, left. We find three cross peaks at coordinates S_W (5,292, 5,219), S_H (5,280, 5,130) and S'_H (5,280, 5,050), caused by the resolution-enhancing characteristic of the asynchronous map. The first cross peak suggests that the silanol groups weakly associated with water molecules are produced in step I_a, since we may assign the bands at 5,292 and 5,219 cm^{-1} to weakly associated SiOH groups and water molecules, respectively. We may assign the bands at 5,050 and 5,130 cm^{-1} to strongly associated water molecules, which are different in the extent of their hydrogen bonds. The appearance of cross peaks S_H and S'_H probably reflects that silanol groups are relatively strongly hydrogen bonded to water molecules.

The sign of cross peak S_W in the asynchronous spectrum is positive and, moreover, the corresponding position in the synchronous spectrum is also positive; therefore, according to the sign rules established for 2D correlation spectra [9], the intensity increase of the 5,292-cm^{-1} band occurs first followed by that of the 5,219-cm^{-1} band. The signs of cross peaks S_H and S'_H are positive in the asynchronous map; however, in the synchronous map, the signs of corresponding positions are negative, indicating that the increase in intensity of the 5,130- and 5,050-cm^{-1} bands occurs after the initial increase in intensity of the 5,280-cm^{-1} band. The cross peaks which arise from the correlation of the silanol band at 5,280 cm^{-1} with ethanol bands (4,650–4,950 cm^{-1}) in the asynchronous map are negative in

sign; however, in the synchronous map, their signs are positive. This observation implies that the intensity increase of the ethanol band occurs first followed by that of the 5,280-cm^{-1} band. The cross peak at coordinates (5,107, 4,748) arise from the correlation between strongly hydrogen bonded water and ethanol molecules.

The synchronous 2D correlation map (step I_b) for the same reaction mixture system is shown in Fig. 3b, top. The connection of the autopeaks at 5,199 and 4,805 cm^{-1} with cross peaks at coordinates (5,199, 4,805) and (4,805, 5,199) provides a correlation square, implying the existence of a correlation (water–ethanol correlation through hydrogen bonding) between the bands at 5,199 and 4,805 cm^{-1}. The presence of the autopeak at 5,199 cm^{-1}, with very strong intensity, reflects the predominant contribution of the correlation of released water with the silanol produced in step I_b.

In the asynchronous map (step I_b) (Fig. 3b, bottom), the strong positive cross peak S'_W arises from the silanol–water correlation (through a relatively strong hydrogen bond) between the bands at 5,288 and 5,157 cm^{-1}. Since the sign of correlation peak at this position is also positive in the synchronous map, the intensity increase of the silanol band at 5,288 cm^{-1} occurs first, followed by that of the water band at 5,157 cm^{-1}. The cross peak at W'_E (5,165, 4,811) may be related to the relatively strong hydrogen-bond network formed between ethanol and water molecules. The sign of this cross peak in the asynchronous map is positive, while that in the synchronous map is negative; thus, the intensity of the water band at 5,165 cm^{-1} increases first, followed by that of the ethanol band at 4,811 cm^{-1}.

The synchronous and asynchronous maps, which were calculated from time-resolved NIR spectra in steps II_a and II_b, are shown in Fig. 4. The synchronous maps (step II_a and II_b) shown in Figs. 4a, top, and 4b, top, in which the correlation patterns are almost similar to each other, consist of an autopeak A ($\nu_1 = \nu_2 = 5{,}172$) and two positive cross peaks B_1 (4,820, 5,172) and B_2 (5,172, 4,820). The extremely strong intensity of autopeak A reflects rapid production of water molecules and silanol groups as a consequence of condensation and hydrolysis reactions. The positive signs of the cross peaks suggest that ethanol molecules are more rapidly released in step II compared to step I.

The asynchronous correlation pattern of step II_a differs from that of step II_b, as seen in Figs. 4a, bottom, and 4b, bottom. In the asynchronous spectrum (step II_a), the cross peaks S_1 and S_2 probably arise from the weakly and strongly hydrogen bonded SiOH versus water OH correlations, respectively. In particular, the existence of cross peak S_1 implies that the formation of silanols also occurs in step II_a. The signs of S_1 and S_2 in the asynchronous map are negative, while those of the corresponding positions in the synchronous map are positive; therefore, the intensity increase of the water band at 5,161 cm^{-1} occurs first, followed by those of the silanol bands at 5,324 and 5,273 cm^{-1}. The two cross peaks Al_1(5,170, 4,829) and Al_2(5,170, 4,760) arise from the correlation between water OH and ethanol OH bands through hydrogen-bonding interaction.

We should note that cross peak S_1 found in step II_a disappears in the asynchronous map (step II_b), and that the cross peak at S'_2 (5,269, 5,165), corresponding to the S_2 peak in the asynchronous map (step II_a), is predominant in this silanol-band area. This correlation peak suggests that most of the silanol groups produced by hydrolysis participate in a relatively strong hydrogen-bonded network with water molecules. The cross peaks at coordinates W'_1 (5,170, 5,060), W'_2 (5,170, 5,018) and W'_3 (5,170, 4,972), which appeared as a consequence of the unique resolution enhancement characteristics of 2D spectra, arise from the correlations among water molecules participating in the hydrogen-bonded networks with different strength. The resolution enhancement also provides at least four cross peaks at coordinates W''_1 (5,170, 4,933), W''_2 (5,170, 4,817), W''_3 (5,170, 4,783) and W''_4 (5,170, 4,694). The water band at 5,172 cm^{-1} correlates with bands coming from ethanol molecules, which participate in the different hydrogen-bonding environments.

Discussion

The growth process of the polymeric precursors can be regarded as the process of polymerization and aggregation that occurs far from equilibrium. Kinetic growth models, which describe these processes, have already been presented for the case of silica polymers [17–20]. Schaffer [19] presented a kinetic model of so-called monomer–cluster (MC) growth and cluster–cluster (CC) growth. This model may be modified to conform to the growth process of the PFO silane polymeric precursors.

The growth mechanism of the PFOTES polymeric precursors, which may be assumed from time-resolved SAXS [4, 5] and NIR data, may be explained as follows. In step I, the acid-catalyzed hydrolysis of the ethoxy portions commences, and consequently, PFO-monohydroxysilane (PFOMHS), PFO-dihydroxysilane (PFODHS) and PFO-trihydroxysilane (PFOTHS) are produced. Subsequently, the formation of dimers occurs. Furthermore, the reaction between monomers and dimers brings about trimers. Thus, the formation of small clusters (i.e., MC growth) becomes predominant in step I. In this step, PFOMHS, PFODHS, and PFOTHS molecules participate equally in the formation of small clusters, resulting in the formation of small clusters with ethoxy groups remaining unreacted. Since the bulky and highly rigid PFO chain provides a marked steric effect for the acid-catalyzed hydrolysis of PFOTES [1, 21], this steric restriction may promote stabilization of ethoxy

groups. Thus, small clusters with unreacted ethoxy groups are predominantly produced in step I. The numbers of unreacted ethoxy groups in step I may be high compared with those in step II.

In step II, it is probable that a condensation reaction between small clusters is predominant, leading to the further growth of small clusters, (i.e., CC growth predominantly occurs in step II). The acid-catalyzed hydrolysis of small clusters with a number of unreacted ethoxy groups brings about the formation of silanols and rapid liberation of ethanol molecules. As a consequence of the condensation reaction between silanols, rapid liberation of water molecules also occurs, resulting in a marked increase in absorbance for the 5,156- and 4,818-cm^{-1} bands in step II.

Furthermore, PFO groups bonded directly to a Si atom have both hydrophobic and lipophobic properties. Therefore, for the growth process of polymeric precursors in the present system, the consequential effect of self-assembly should be considered. The Guinier radius obtained from the recent SAXS study for the same reaction system points to an aggregation number of 2 for PFOTES in ethanol, indicating that even PFOTES monomers form dimers in ethanol. Furthermore, in our previous study [4], using time-resolved ^1H NMR spectra, we confirmed the high population of PFOTES monomers in the initial step. The present result may be regarded as another indication of the effect of self-assembly between the monomer (PFOTES) and a small cluster.

Thus, small aggregates consisting of PFOTES MC complexes may be predominantly present in step I. Ethoxy groups remaining unreacted in small aggregates are further hydrolyzed by acid catalysis, and then reactive small aggregates with silanol groups are rapidly produced after liberation of ethanol. The condensation reaction between reactive small aggregates brings about liberation of water molecules.

We should note the mechanism of cluster growth in the second step in connection with the mechanism of the sol–gel transition. In fact, Brinker et al. [1] noted the existence of polymeric structures weakly cross-linked with each other in the tetraethoxysilane–alcohol system. This idea may be applied to the growth process in step II, in which the polymeric structures will initially be weakly cross-linked with each other, until finally, after extensive cross-linking has occurred, phase separation into a solvent-rich upper layer and a polymer-rich bottom layer will occur.

It is difficult to discuss the dynamic variation of silanols using the time-resolved NIR spectra since the time-dependent absorbance data of the SiOH band at about 5,300 cm^{-1} are extremely small and not easily distinguished from those for the water bands at 5,150–5,200 cm^{-1}. However, the 2D NIR correlation map provides direct information on the dynamic behavior of silanol groups.

In our previous work [14], we presented the 2D NIR correlation maps of the PFOTES–ethanol system catalyzed by a low HCl concentration (0.25 M). In the 2D correlation maps, we ascribed the bands at 5,340 and 5,253 cm^{-1} to weakly associated and strongly associated SiOH groups, respectively. In the synchronous map (step I_a) of the PFOTES–ethanol–1.0 M $HCl{\cdot}H_2O$ system (Fig. 3a, top), we may assign the band at 5,280 cm^{-1}, which leads to autopeak A_1, to relatively strongly associated SiOH groups. The extremely strong intensity of autopeak A_1 reflects that the silanol groups, predominantly produced in step I_a, may be stabilized by interaction with water, ethanol, and silanol itself through hydrogen bonding.

The formation of weakly or strongly associated SiOH groups may be caused by self-assembly of aggregates. The steric restriction of the PFO chains probably promotes isolation of any silanol groups which may be incorporated into the grooves of aggregates formed by PFO chains. Thus, the environment of the PFO chains may be closer to the hydrophobic and lipophobic regions, bringing about the formation of weakly associated silanols. However, most of the silanol groups which participate in the associated silanol groups probably form a hydrogen-bonding network with SiOH itself, or water or ethanol molecules. The existence of cross peaks C_1, C_2, and B_2 may provide evidence that silanol groups form the association system with silanol itself, or with water or ethanol.

In particular, in the asynchronous map (I_a), as a consequence of the resolution-enhancing effect, cross peak S_w provides evidence for a weakly associated system between silanol and water molecules. Furthermore, cross peaks S_H and $S_H^{'}$ may imply that a strongly associated system between silanol and water also exists.

In step I_a, the amount of water released must be small compared with that of the silanols produced, leading to the separate observation of autopeaks A_1 and A_2. The result made it possible to discuss the interaction modes among silanol, water, and ethanol. In step I_b, the amount of water released becomes larger compared with that in step I_a; therefore, the correlation peaks arising from various interaction modes must be averaged in the synchronous map (step I_b). For example, the wavenumber, 5,199 cm^{-1} (or 4,805 cm^{-1}), of the water (or ethanol) band is very close to the average value, 5,194 cm^{-1} (or 4,805 cm^{-1}), of the wavenumbers of the bands at 5,107 and 5,208 cm^{-1} (or those at 4,748 and 4,860 cm^{-1}) appearing in the synchronous map (step I_a). In the asynchronous map (step I_b), the very strong correlation of the silanol band at 5,288 cm^{-1} with the water band at 5,157 cm^{-1} is predominant, and the very weak intensity of cross peaks S_{Al} and W_S may imply that the interaction between silanol and alcohol (or water and water) is very small.

We emphasize that the cross peaks W_i' ($i = 1$–3) and W_i ($i = 1$–4) arising from the water–water and water–ethanol interaction modes appear predominantly in step II, although the amount of water and ethanol released becomes larger than in step I. This result suggests that during the polymerization process in step II, the hydrogen-bonding environment of silanol, water, and ethanol changes in a two-step process, in which small oligomeric aggregates are formed in step I, and the formation of larger polymeric aggregates occurs in step II. Therefore, we may assume that the size of the hydrogen-bonding network and the strength of the hydrogen bonds may be different between steps I and II.

Conclusion

The time-resolved NIR spectra of the PFOTES–ethanol–HCl·H_2O (0.5, 1.0 and 2.0 M) systems were measured on the time scale of 10–240 min. The results demonstrated that the growth process of the polymeric aggregates occurs in two steps, and that a high HCl concentration decreases the time for commencement of the second step.

In order to examine the microstructural variation of the polymeric aggregates in a two-step process, 2D NIR correlation spectra were calculated from time-sliced NIR data collected in each step. It was found that the 2D NIR correlation maps directly reflect variation of the interaction among silanol, water, and ethanol in the reaction process, related to the size of the aggregates in each step.

Acknowledgement We sincerely thank Akishi Nara of Osaka Laboratory, Nicolet Japan, for helpful NIR measurements.

References

1. Brinker CJ, Keefer KD, Schaefer DW, Ashley CS (1982) J Non-Cryst Solids 48:47
2. Einaga H (2000) In: Inorganic synthesis in solution as a reaction field. Baifukan, Tokyo, p 169
3. Jönsson B, Lindman B, Holmberg K, Kronberg B (1998) In: Surfactants and polymers in aqueous solution. Wiley, Chichester, p 31
4. Ogasawara T, Izawa K, Hattori N, Okabayashi H, O'Connor CJ (2000) Colloid Polym Sci 278:293
5. Izawa K, Ogasawara T, Okabayashi H, Monkenbusch M, O'Connor CJ (2001) Colloid Polym Sci (submitted)
6. Noda I (1986) Bull Am Phys Soc 31:520
7. Noda I (1989) J Am Chem Soc 111:8116
8. Noda I (1990) Appl Spectrosc 44:550
9. Noda I (1993) Appl Spectrosc 47:1329
10. Ozaki Y, Liu Y, Noda I (1997) Appl Spectrosc 51:526
11. Ozaki Y, Noda I (1996) J Near-Infrared Spectrosc 4:85
12. Ren Y, Murakami T, Nishioka T, Nakashima K, Noda I, Ozaki Y (2000) J Phys Chem B 104:679
13. Ogasawara T, Nara A, Okabayashi H, Nishio E, O'Connor CJ (2000) Colloid Polym Sci 278:1070
14. Ogasawara T, Nara A, Okabayashi H, Nishio E, O'Connor CJ (2000) Colloid Polym Sci 278:946
15. Izawa K, Ogasawara T, Masuda H, Okabayashi H, Noda I (2001) Macromolecules (in press)
16. Izawa K, Ogasawara T, Masuda H, Okabayashi H, Noda I (2001) Phys Chem Commum 12:1
17. Witten TA, Cates ME (1986) Science 232:1607
18. Sander LM (1987) Sci Am 256:94
19. Schaefer DW (1989) Science 243:1023
20. Daoud M, Family F (1984) J Phys Lett 45:L151
21. Scheafer DW, Keefer KD (1986) Mater Res Soc Symp Proc 73:277